the spectrum obtained on hydrogen abstraction from **18** and simulations with equal and statistical proportions of the three methylcubyl radicals; EPR spectrum of the tricyclo allyl radical **6**; a plot of the measured activation energies for β-scission of cyclo- and polycycloalkylcarbinyl radicals against relief of ring strain ΔSE; and a listing of crystal and structural data for *cis,cis*-3,4,7,8-tetrabromo-*syn*-tricyclo[4.2.0.$0^{2,5}$]octane (**30**) (12 pages). Ordering information is given on any current masthead page.

An Axiomatic Model of the Intramolecular Diels–Alder Furan Reaction

Daniel P. Dolata*,† and Laurence M. Harwood‡

Contribution from the Department of Chemistry, University of Arizona, Tucson, Arizona 85721, and Dyson Perrins Laboratory, University of Oxford, South Parks Road, Oxford OX1 3QY, U.K.
Received May 26, 1992

Abstract: An axiomatic model has been created for the intramolecular Diels–Alder furan (IMDAF) reaction. The model is based on the energetics of implicit transition states, which are deduced from explicit starting material and product conformations. These explicit conformations are obtained by a combination of the WIZARD and MM2 programs. The model gives good quantitative agreement for 15 out of 16 IMDAF reactions and affords a good qualitative agreement for the remaining reaction. In several cases, the model was used to make predictions about as yet untried reactions, and in all but one case, the model was successful in predicting the results of the reactions. The technique of implicit transition-state modeling is not based on any specific characteristics of the IMDAF reaction and should provide a new and rapid method for modeling many classes of reactions.

Introduction

The intramolecular Diels–Alder (IMDA) reaction provides an excellent method for constructing complex ring systems with good stereocontrol.[1] However, the reaction is not as simple as it might appear at first glance.[2] In many cases, it is neither purely kinetically controlled nor thermodynamically controlled, although it is often reversible and is capable of giving a mixture of endo and exo products (the reactions of furans with dieneophiles, for instance). Intermolecular DA reactions of normal dienes generally occur under kinetic conditions and furnish the endo product. This has been explained by utilizing a mixture of frontier molecular orbital (FMO) theory and steric considerations.[1b,3] FMO theory says that the transition state leading to the endo product gains increased stabilization due to favorable nonbonding orbital overlap, while steric considerations generally direct the exo product to be less sterically hindered and, therefore, more stable.

The analysis of intramolecular Diels–Alder reactions is more complex, since one has to take into account not only the relative stabilities of the endo and exo products and the stabilizing effect of FMO overlap on the transition state but also the ability of the connecting chain to fold into the required conformation found in the transition state, as shown in Figure 1 (based on a figure from Roush et al.).[4a] Since the reaction is complicated, an exhaustive theoretical analysis of the intramolecular Diels–Alder reaction would require substantial effort. If the reaction went to thermodynamic equilibrium, all that a model would require would be the determination of the full ensemble of all product conformations, the calculation of their relative energies, and the utilization of the Boltzmann distribution to predict the product ratios. However, many (if not most) DA reactions are not run to strict thermodynamic completion in the laboratory. One example of this can be found in the studies of Roush.[4] When Roush performed the intramolecular DA reactions at temperatures ranging from 150 to 180 °C for time periods ranging from 5 to 40 h in the absence of catalysts, he received trans:cis product ratios ranging from 60:40 to 72:28. When aluminum catalysts were used, the reactions proceeded easily near room temperature, thermodynamic equilibrium was achieved, and the product ratios changed dramatically in all but one case. Other DA reactions have been reported to change their product ratios when performed under conditions of acid catalysis.[2b] Partial or complete kinetic control of the Diels–Alder reaction is also found in Houk's studies of transition-state energies of the reactions of nonatriene and decatriene. Houk found a "qualitative agreement with experimental trends".[4] Since product ratios are controlled by transition-state energies in kinetic reactions, this suggests a significant amount of kinetic control.

Recently one of us (L.M.H.) has been studying the intramolecular Diels–Alder furan reaction (IMDAF) as a means for the stereospecific construction of 7,6-fused carbobicycles with a view toward developing methodology for phorbol and daphnane syntheses.[5] The reactions do not normally proceed at room pressure but can be accelerated by the application of high (5–19

† University of Arizona.
‡ University of Oxford.

(1) (a) Blokzijl, W.; Blandamer, M. J.; Engberts, J. B. F. N. *J. Am. Chem. Soc.* **1991**, *113*, 4241. (b) Breiger, G.; Bennet, J. N. *Chem. Rev.* **1980**, *80*, 63. (c) Jung, M. E.; Gervay, J. *J. Am. Chem. Soc.* **1991**, *113*, 224. (d) Keay, B. A.; Dibble, P. W. *Tetrahedron Lett.* **1989**, *30*, 1045. (e) Rogers, C.; Keay, B. *Tetrahedron Lett.* **1989**, *30*, 1349. (f) Keay, B. *J. Chem. Soc., Chem. Commun.* **1987**, 419. (g) Jung, M. E.; Truc, V. C. *Tetrahedron Lett.* **1989**, *29*, 6059. (h) Sauer, J.; Sustmann, R. *Angew. Chem., Int. Ed. Engl.* **1980**, *19*, 779. (i) Fallis, K. *Can. J. Chem.* **1984**, *62*, 183.

(2) (a) Jung, M. *Synlett* **1990**, *4*, 186. (b) Rogers, C. *Synlett* **1991**, *5*, 353. (c) Jung, M. E.; Gervay, J. *J. Am. Chem. Soc.* **1989**, *111*, 5469. (d) Jung, M. E.; Gervay, J. *Tetrahedron Lett.* **1988**, *29*, 2429. (e) Houk, K. N.; Paddon-Row, M. N.; Rondan, N. G.; Wu, Y.; Brown, F. K.; Spellmeyer, D. C.; Metz, J. T.; Li, Y.; Loncharich, R. J. *Science* **1986**, *231*, 1108. (f) Boeckman, R. K., Jr.; Ko, S. S. *J. Am. Chem. Soc.* **1980**, *102*, 7146. (g) White, J. D.; Sheldon, B. G. *J. Org. Chem.* **1981**, *46*, 2273. (h) Dewar, M. J. S.; Pierini, A. B. *J. Am. Chem. Soc.* **1984**, *106*, 209.

(3) Fukui, T. *Ang. Chem., Int. Ed. Engl.* **1982**, *21*, 801.

(4) (a) Roush, W. R.; Gillis, H. R.; Ko, A. I. *J. Am. Chem. Soc.* **1982**, *104*, 2269. (b) Brown, F. K.; Houk, K. N. *Tetrahedron Lett.* **1984**, *25*, 4609.

(5) (a) Harwood, L. M.; Iszhikawa, T.; Phillips, H.; Watkin, D. *J. Chem. Soc., Chem. Commun.* **1991**, 527. (b) Harwood, L. M.; Jackson, B.; Jones, G.; Prout, K.; Thomas, R.; Witt, F. *J. Chem. Soc., Chem. Commun.* **1990**, 609. (c) Harwood, L. M.; Jones, G.; Pickard, J.; Thomas, R. M.; Watkin, D. *J. Chem. Soc., Chem. Commun.* **1990**, 605. (d) Harwood, L. M.; Jones, G.; Pickard, J.; Thomas, R. M.; Watkin, D. *Tetrahedron Lett.* **1988**, 5825. (e) Harwood, L. M.; Leeming, S. A.; Isaacs, N. S.; Jones, G.; Pickard, J.; Thomas, R. M.; Watkin, D. *Tetrahedron Lett.* **1988**, 5017.

0002-7863/92/1514-10738$03.00/0

Table I. Summary of Reaction Results

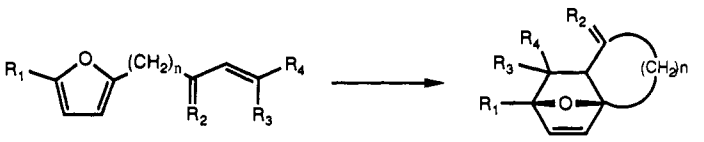

N

Na(endo)
Nb(exo)

n	R_1	R_2	R_3	R_4	*n*	*P* (kbar)	endo **Na**	exo **Nb**	notes
1	H	H	H	CH_3CO	3	10	**1**	**3**	
1	H	H	H	CH_3CO	3	19	**2**	**7**	18% SM[h]
2	H	H	CH_3CO	H	3	10	**1**	**3**	75% SM
2	H	H	CH_3CO	H	3	19	**1**	**5**	53% SM
3	CH_3	H	H	CH_3CO	3	10			
3	CH_3	H	H	CH_3CO	3	19	**1**	**19**	
4	CH_3	H	CH_3CO	H	3	10		*a*	
5	H	O	H	H	2	19			
6	H	O	H	H	3	19	**1**	**18**	
7	H	O	H	H	4	12	**1**	**1**	*b*
8	CH_3	O	H	H	2	19			
9	CH_3	O	H	H	3	10		**1**	
10	CH_3	O	H	H	4	12		**1**	*b, c*
10	CH_3	O	H	H	4	12	**1**	**1**	*b, d*
10	CH_3	O	H	H	4	12	**7**	**3**	*b, e*
11	CH_3	O	H	CH_3CO	2	19			
12	CH_3	O	H	CH_3CO	3	1		**1**	40% SM
12	CH_3	O	H	CH_3CO	3	19		**1**	
13	CH_3	O	H	CH_3CO	4	10	**1**		50% SM
13	CH_3	O	H	CH_3CO	4	19	**5**	**1**	25% SM
14	CH_3	O	CH_3CO	H	2	19	trace	trace	
15	CH_3	O	CH_3CO	H	3	1			
15	CH_3	O	CH_3CO	H	3	19		*f*	
16	CH_3	O	CH_3CO	H	4	10	**1**		35% yield, *g*
16	CH_3	O	CH_3CO	H	4	10	**1**		12% SM

[a] Epimerizes to product from **3**. [b] Cycloreversion at 1 bar. [c] Reaction time = 1 h. [d] Reaction time = 8 h. [e] Reaction time = 50 h. [f] Product epimerizes to product from **12**. [g] Product was hydrogenated to prevent epimerization, and yield is based on hydrogenated product. [h] SM = starting material.

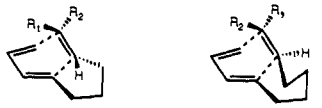

A B

Figure 1. Endo versus exo IMDA reactions of substituted 1,3,8-nonatrienes (after Roush).

kbar) pressure.[5e] The products of these reactions can be either the exo or the endo adducts, and at least one reaction has demonstrated a product ratio that is time dependent. The results of these experimental studies are summarized in Table I. This paper reports on our theoretical studies of this reaction.

Results and Discussion

Early Studies. We initially attempted to model the IMDAF reaction on simple thermodynamic grounds. We utilized our conformational search program WIZARD[6] to generate all of the conformations of the endo (**Na**) and exo (**Nb**) products for each reaction. WIZARD is a logic-based theorem proving program that uses an axiomatic theory of conformational analysis to rapidly and accurately search the conformational space of molecules. However, while WIZARD is capable of predicting *structure*, it is not as good as MM2 in calculating *energy*. Thus, it is desirable to utilize a numerically based (as opposed to logically based) program to obtain the energies on the basis of WIZARD's structural predictions. For this study we utilized MM2. In other studies, such as our work on nucleophilic additions to carbonyls,[7] we have utilized MOPAC. This combination of using a rapid search program followed by an accurate numerical program has been shown to be more productive than utilizing the relatively simple conformational search methods implemented in most numerical programs (e.g., torsion angle driving[6a,8]). The strain energies of the most stable conformers are shown in Table II, along with the experimental product ratios. While the product ratios are in general agreement with the relative strain energies for nine

Table II. Most Stable Product Conformers, As Found by WIZARD

	exptl product ratio		calcd MM2 Strain		calcd	
N	**Na** endo	**Nb** exo	**Na** endo	**Nb** exo	ΔH_{strain}	notes
1	**2**	**7**	34.6	32.1		
2	**1**	**5**	36.8	32.6		
3	**1**	**19**	36.8	33.8		
4	**2**	**3**[a]	36.6	35.2		
5			44.8	34.8	20.2	*a*
6	**1**	**18**	33.8	30.9	15.9	
7	**1**	**1**	34.9	36.1	20.1	*b*
8			44.5	34.6	18.7	*a*
9		**1**	33.5	30.7	14.3	
10	**1**	**1**	34.6	35.8	17.9	*b, c*
11			47.1	36.3	18.1	*a*
12		**1**	35.9	31.4	12.8	
13	**5**	**1**	37.0	36.7	17.8	*b*
14	trace	trace	48.8	38.0	21.4	*a*
15		*d*	36.6	35.6		
16	**1**		38.1	39.8	10.5	

[a] Exo product is more stable than other observed products, yet no reaction. [b] Calculated ΔH difference between product is not commensurate with experiment. [c] Time dependency of endo:exo ratio is not accounted for by simple thermodynamics.

(6) (a) Dolata, D. P.; Carter, R. E. *J. Chem. Inf. Comput. Sci.* **1987**, *27*, 36. (b) Leach, A. R.; Dolata, A. R.; Prout, K. *J. Chem. Int. Comput. Sci.* **1990**, *30*, 316. (c) Leach, A. R.; Prout, C. K.; Dolata, D. P. *J. Comput. Chem.* **1990**, *11*, 680.

(7) Dolata, D. P.; Spina, D. R.; Mash, E. A. *Tetrahedron Lett.* In Press.

(8) Burkert, U.; Allinger, N. L. *J. Comput. Chem.* **1982**, *3*, 40.

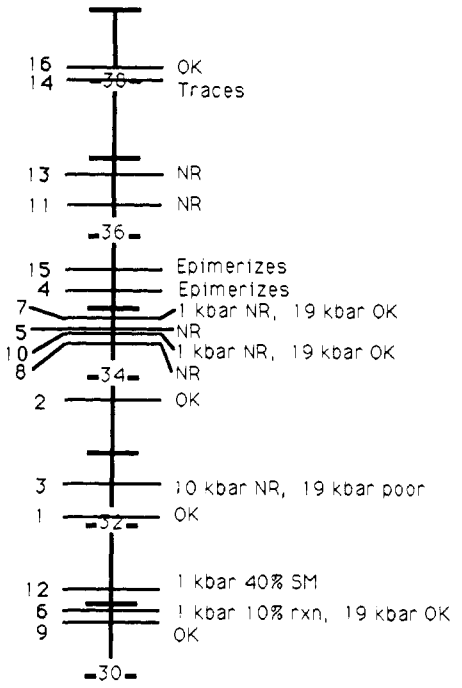

Figure 2. Calculated strain energy (MM2) of the most stable conformation for the product of each IMDAF reaction displayed on an "energy ladder" labeled in kcal/mol. Height on the ladder does not correlate well with reactivity. OK = clean formation of product, NR = no reaction.

of the reactions (those of **1–4**, **6**, **9**, **12**, **15**, and **16**), this data cannot be used to explain seven of the reactions (**5**, **7**, **8**, **10**, **11**, **13**, and **14**). For example, in the reaction of **13** the product **13b**, which is predicted to be only slightly more stable (**13b**, 36.7 kcal/mol, **13a**, 37.0 kcal/mol), is formed in far smaller amounts (20%) than the difference in product strain energy would account for, while in the reactions of **7** and **10** the experimentally observed 1:1 product ratios do not reflect the much larger (1.2 kcal/mol) energy differences in calculated product strain energies (e.g., **7a** = 34.9 kcal/mol, **7b** = 36.1 kcal/mol).

The calculated strain energies for the most stable product conformations cannot be used to explain the equilibrium direction of the reactions either. This is shown in Figure 2. While there is a vague correlation, several of the reactions (those of **5**, **8**, **11**, **13**, and **14**) do not afford products under the experimental conditions yet are predicted to be less strained than those reactions in which products are observed (e.g., **5b** = 34.8 kcal/mol and is not observed vs **7a** = 34.9 kcal/mol or **7b** = 36.1 kcal/mol). In retrospect this was not surprising, since the equilibrium of a reaction is determined by ΔH_f of the starting materials and products instead of the absolute H_f or absolute H_{strain} of the products alone. We utilized WIZARD/MM2 to find the strain energies for the global minimum conformations for 11 of the 16 reactions (these values are shown in column 6 of Table II). The value of ΔH_f is related to ΔH_{strain} through the equation $\Delta H_f = \Delta H_{nonstrained} - \Delta H_{strain}$. If we assume that $\Delta H_{nonstrained}$ is similar for each reaction in a homologous series of reactions (e.g., those of compounds **5–7**, **8–10**, etc.), then we can infer that ΔH_{strain} will be linearly proportional to ΔH_f within that set of reactions. The relative values of ΔH_{strain} (and by inference, ΔH_f) still do not adequately explain the equilibrium direction within a homologous set of reactions (cf. Table II). Compound **7** gives a good yield of **7a** and **7b** with a calculated ΔH_{strain} of 20.1 kcal/mol, while the unsuccessful reaction of the homologous compound **5** to give **5b** is calculated to require only 20.2 kcal/mol. Similar behavior was observed in other homologous pairs (**8**,**10**, **11**,**13**, and **14**,**16**). Thus, it seemed impossible to explain either the product ratios or the direction of equilibrium for these reactions on thermodynamic grounds alone.

We also investigated the possibility that the direction and reversibility of the reaction and the product ratios could be controlled by the relative molar volumes of the products. The experimental and theoretical molar volumes of some starting materials and products are shown in Table III. The agreement between the experimentally determined volumes[9] and the calculated volumes for **10**, **10a**, and **10b** is within 2%. In all of the reactions, the products have smaller volumes than the starting materials, which is commensurate with the requirement for high pressure in the IMDAF reaction. However, there is insufficient correlation between the relative volumes and either the product ratios or the success of the reaction for this to be the major controlling factor. For example, the reaction **6** to **6b** shows a decrease of only 3 cm^3 mol^{-1} and proceeds to completion, while both **11** and **14** show greater decreases in volume but do not give appreciable amounts of product. The relative volumes of the products cannot explain the experimentally obtained product ratios, either. The molar volumes of **12a** and **12b** are calculated to be equal, and those of **15a** and **15b** are nearly so, yet only the exo (b) products are obtained in these reactions. On the other hand, the smaller molar volume of **6a** could possibly combine with the greater stability of **6a** to help promote the formation of this product under conditions of higher pressure and longer reaction time. Thus, we concluded that while relative molar volumes might be a contributing factor, the main sources of control for this reaction must lie in another direction.

Table III. Calculated and Experimental Molar Volumes of Some Starting Materials and Products

	theoretical[a] (cm^3 mol^{-1})			experimental (cm^3 mol^{-1})			
compd	SM[b]	endo prod	exo prod	SM	endo prod	exo prod	notes
6	145	140	142				exo only
10	181	164	171	183	164	169	endo/exo time dependent
11	176	170	168				NR[c]
12	190	183	183				exo only
14	177	169	172				NR/traces
15	191	187	186				exo only

[a] The volume of the most stable conformation is shown. The volumes of all conformations within 3 kcal of the most stable conformation were checked and were found to be within 2% of that shown. [b] SM = starting material. [c] NR = no reaction.

Our failure to model the IMDAF reaction on the basis of purely thermodynamic grounds did not surprise us. Other studies have shown that most DA reactions run under conditions of partial kinetic control. The fact that the **10a**:**10b** product ratio was time dependent demonstrated that at least one example of the IMDAF reaction contained an appreciable kinetic component. Thus, we needed to construct a model which took into account both the thermodynamic and the kinetic factors of this reaction. To do this, we would have to consider the enthalpies of the conformational ensembles of the starting materials, products, and corresponding transition states. This knowledge would allow us to estimate the relative rates of each reaction. We considered obtaining the energies of the transition states by utilizing a saddle-point calculation or reaction path calculation in either a semiempirical or an ab initio method. While this is hypothetically possible, in practice semiempirical methods have been shown to have problems in modeling cyclic transition states,[2] and the use of ab initio techniques utilizing good basis sets would be computationally impossible for so many large molecules. Houk's use of ab initio techniques to create MM2 parameters to model transition states has great potential, but his work on the Diels–Alder reaction has focused on hydrocarbon dienes and dienophiles. Since MM2 requires accurate parameterization to give good results, especially with regard to energies, it seemed unlikely that these parameters would be sufficiently analogous to give good results with aromatic furanyl dienes and activated dienophiles. Thus, we needed to find other method. Since we have substantial experience in creating and using axiomatic systems (our conformational analysis program WIZARD is an axiomatic theorem prover), we decided to create an axiomatic theory for modeling the IMDAF reaction.

(9) Harwood, L. M.; et al., manuscript in preparation.

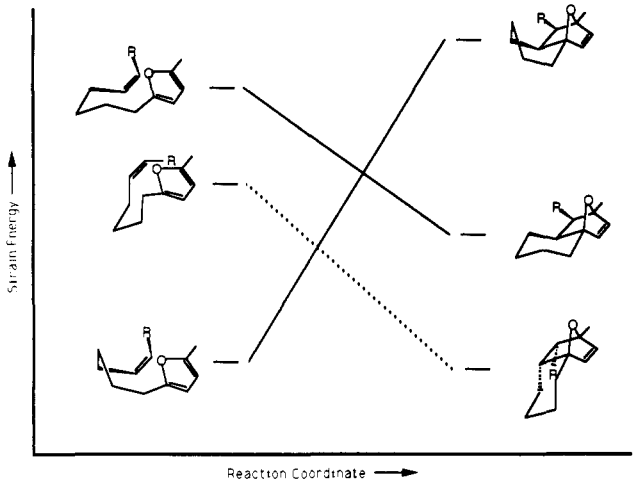

Figure 3. The Toreva program uses rms distance matching on the non-hydrogen atoms to find correlations between starting material (SM) and products and creates correlation lines for matching pairs.

The Axiomatic Model. An axiomatic theory is comprised of a set of defined terms, a series of assumed truths about the terms and their relations (axioms), and rules of inference. These yield a (possibly infinite) series of sentences which *logically follow* from the terms and axioms. Examples of axiomatic theories include Euclidian geometry, group theory, and quantum mechanics. An axiomatic theory per se is a purely formal construct. The utility of axiomatic systems arises when one creates a *model* of physical reality by defining an *interpretation* of the terms and sentences. If the model agrees with and predicts physical reality as we perceive it, we can then describe the model as being useful. Thus, our goal was to create a useful model for the IMDAF reaction on the basis of a formal axiomatic theory. We then checked the utility of the model by making predictions for as yet untried IMDAF reactions, performing those reactions, and then comparing the results to the model. The following axioms were used for this model.

(1) We assumed that the conformation of the "uninvolved atoms" (i.e., those atoms that are not part of the minimal six-atom DA reaction) would generally remain constant during the reaction. While we expect rapid conformational equilibrium before and after the reaction, we expect that the conformation of the uninvolved atoms in the starting material will correspond to their conformation in the product (vida infra). We looked for such correspondences between the sets of starting conformations and product conformations and associated each line of correspondence with a single reaction pathway and thus with a single unique transition state.

(2) We assumed that the transition-state geometry for the "involved atoms" (i.e., the six atoms of the diene and ene) for each pathway would be similar to the transition-state geometries for all other pathways in *the same reaction* and would occur at approximately the same distance along the reaction coordinate. While we know that the electronic structure of the transition state will be somewhat sensitive to the conformation of the electronically "uninvolved" portions of the molecule, it is unlikely that a charge in conformation would shift an early transition-state geometry to a late transition-state geometry, for example.

(3) We assumed that the transition state for the "normal" Diels–Alder reaction is an early-to-middle transition state (in other words, bond formation has proceeded to about the same extent as bond cleavage). An early transition state is in agreement with the known exothermicity of most DA reactions, the experimental evidence given by Roush, the transition-state model created by Houk, and the Alder rule. On the other hand, the IMDAF reaction is likely to have a middle or late transition state, since the reaction is not exothermic, needs forcing conditions to proceed, and in some cases undergoes spontaneous reversion.

(4) We assumed that the height of the transition state above the line of correspondence is approximately equal for all pathways. We assumed that at worst the heights would be proportional and

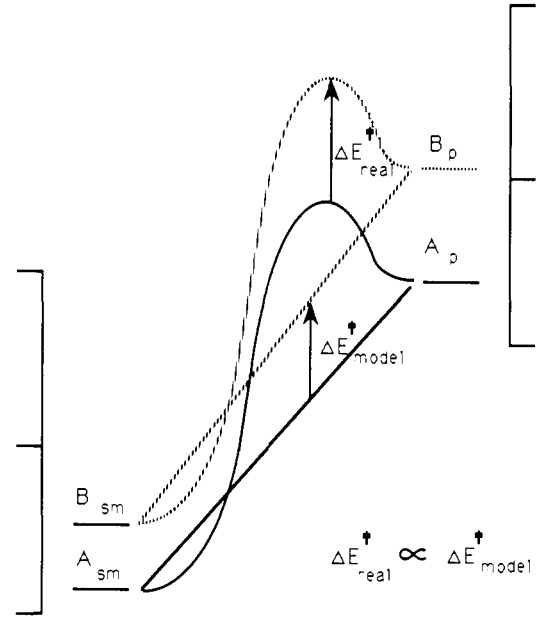

Figure 4. Use of the correlation lines between starting material (SM) and products to estimate the transition-state energies.

that if the correspondence line B of pathway B lay above the correspondence line A for another pathway A at the assumed position of the transition state, then transition state B would be more energetic than transition state A (cf. Figure 4).

(5) We assumed that the ΔH_f of any conformer is a function of the strain energy ΔH_{strain} (determined by MM2) combined with a hypothetical $\Delta H_{nonstrained}$ term based on the Δ_H of making and breaking bonds in a hypothetical strain-free environment. We assume that the latter is constant for the different pathways of the same reaction; thus, the relative ΔH_f for any pathway is directly related to the relative $\Delta H_{strain\ prod} - \Delta H_{strain\ SM}$.

Our first axiom is based on the idea that the reaction itself and any possible conformational changes at the uninvolved atoms are independent events. If they are truly independent, then the energy for performing both at once will be approximately a linear summation of the individual energies. Thus, a simultaneous reaction and conformational change of the uninvolved atoms will exhibit a higher $\Delta E^{\ddagger}$ and will be a substantially slower process compared to a pathway in which the two events occur in succession (pre- or postreaction conformational equilibrium). This assumption might fail if the change in the transition-state geometry of the involved atoms acts on the conformation of the uninvolved atoms so that these atoms are not truly independent of the transition-state geometry or if the conjugated systems of the activated dienophiles are sufficiently distorted so as to change the electronic properties of the dienophile. In such cases, a concomitant change in the conformation of the uninvolved atoms could lower the transition-state energy of the reaction so that combined events are energetically more favorable than sequential events. However, this latter explanation is more complicated than the assumption that the events are independent, and so we utilized the principle of William of Occam's razor (i.e., choose the simplest explanation) to postpone consideration of this more complex possibility until such time as the simpler axiom of independence fails to yield a viable model of the reaction. We will show that the complex axiom is not needed for adequately explaining the IMDAF reaction.

The first axiom required that we consider all of the conformations of the starting material (SM) and the products for the reaction and find correlations between them. We had already utilized WIZARD to obtain the sets of product conformations for our previous unsuccessful attempts at modeling the reaction. Since we were only interested in those starting material conformations which corresponded to a product, we constrained WIZARD to generate only those conformations in which the terminal atoms of the diene were within 3.5 Å of the dienophile. While these conformations will be from 3 to 10 kcal/mol more strained

than the extended conformations and thus will be only sparsely populated, the Curtin–Hammett principle states that we should observe reactions from these conformations, if there is a sufficiently rapid preequilibrium between these conformations.[10] Since the energy of activation for the DA reaction is estimated to be about 25–30 kcal/mol[4b] and the barriers to conformational change among these conformers should be less than 3–10 kcal/mol, the Curtin–Hammett conditions should be satisfied.

Once we had ensembles of conformations for each starting material and its endo and exo products, we utilized a second program (called TorEva) to find correspondences between each product and a starting material conformation. This is shown schematically in Figure 3. This information was used to create a "correspondence diagram" which links each product conformation to the corresponding starting material. As TorEva examined each potential correspondence, it rejected the match if any single torsion angle difference or the sum of all torsion angle differences in the uninvolved bonds exceeded certain cutoff values. TorEva found that some SM or product conformations did not correspond to any conformations on the other side of the reaction. These conformations could take part in the reaction if they underwent the previously rejected simultaneous reaction and conformational change, but in this study they were assumed to be "orphaned" and were not considered further when the reaction pathways were assigned. Fortunately, none of the low-energy SM conformations which met the distance constraint and none of the low-energy product conformations were orphans. We do not know if this was serendipitous or if this might somehow mirror a general property of successful reactions. We did notice (but did not study) the fact that the worst reactions seemed to exhibit a greater number of orphans than the reactions which cleanly and easily afforded products. Since WIZARD has been shown to normally provide excellent coverage of the conformational possibilities for this type of molecule, this must reflect a requirement for substantial conformational change and deformation during the reaction. This would add to the energy of the transition state (TS) and could explain why these reactions are slower.

The second, third, and fourth axioms determine how we model the energy of the transition state, as shown in Figure 4. Once the correspondence diagrams had been drawn for each reaction, the position of the transition state along the reaction coordinate was estimated following axioms 2 and 3. We began by assuming that the transition state would be at 50–60% along the reaction coordinate. The Hammond postulate states that the position of the TS will shift as a function of the relative energies of the SM and the products. However, since the position of the transition state was only being estimated in a qualitative fashion, we did not attempt to create a formula which calculated $TSx_{\text{reaction coordinate}}$ as a function of ΔH_f. As we will show, adjustment of the position of the transition state away from a rough midpoint was useful (and even then not strictly required) in only one case. We then used the fourth axiom to compute the relative transition-state energies. This axiom states that all of the transition states for each individual conformational pathway in the same reaction will be approximately the same height above the correspondence line. Since this is a constant increment, we can simply examine the relative heights of the correspondence lines at the estimated position of the transition state. This allows us to obtain an estimated $\Delta E^{\ddagger}_{\text{model}}$ of the relative rates for each pathway, which should be proportional to the actual $\Delta E^{\ddagger}_{\text{real}}$.

Results

The axiomatic model was constructed during early phases of the study of the IMDAF reaction, when only medium pressures ($p \leq 12$ kbar) had been applied to a limited number of reactions. The model was checked against these early results, and it showed qualitative agreement in most cases. In these cases only the results of the later experiments are tabulated and discussed. However, in a few cases the model was either in partial or complete disagreement with the experimental results. These cases are noted below, and the results of both the early and later experiments are tabulated and discussed.

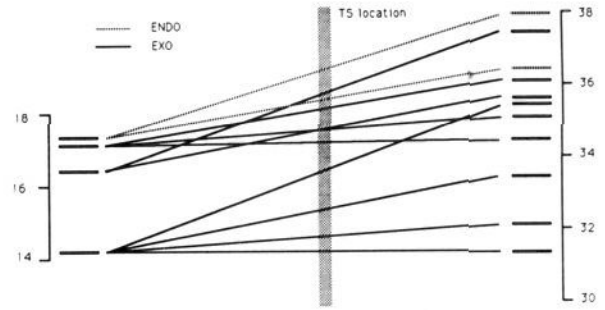

Figure 5. Correlation diagram for the reaction of compound **12**. Only the exo product is observed experimentally.

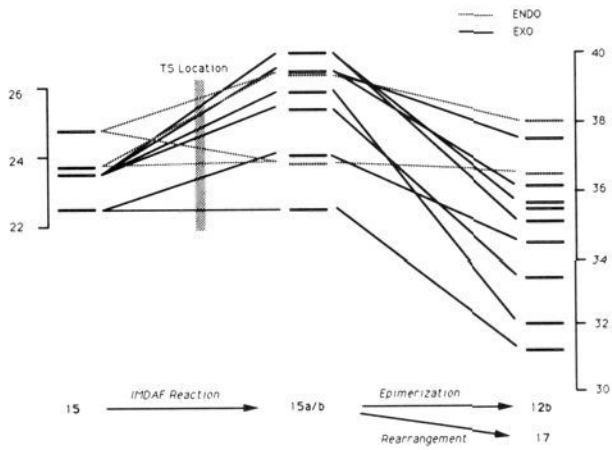

Figure 6. Correlation diagram for the reaction of compound **15**. Products **15a** and **15b** are not observed, since they are highly strained and have facile rearrangement pathways.

To illustrate how we interpreted the correlation diagrams, we will begin with a few simple examples and work toward the more complex examples. The set of doubly activated Diels–Alder reactions of compounds **11**–**16** is a good place to begin, since the interpretation of the correlation diagrams is fairly straight forward. The correlation diagram for the reaction of **12** is shown in Figure 5. The starting material conformations which lead to the exo products are all more stable than those which lead to the endo products. In addition, the exo products are much more stable than the endo products. Given the axioms, we can infer that the transition states leading to the exo products should be substantially lower in energy (~4 kcal/mol) than the transition states leading to the endo products. Thus, we would expect that the exo product would be the predominant product (>99.9%) on either kinetic or thermodynamic grounds. This explanation is commensurate with the experimental results that only the exo product was observed.

The correlation diagram for the related cis dienophile **15** is shown in Figure 6. The diagram contains two reactions: the left half shows the IMDAF reaction, while the right half shows an epimerization of the ring juncture proton. Based on the model, we predicted that we would see the exo product **15b** predominate in the IMDAF reaction, with some smaller amount of **15a**. In fact, **15b** was originally observed as the exclusive product via its rearrangement product; reaction at 10 kbar led to the initial product **15b** which epimerized to give the exo product **12b**. This can be understood if we compare the relative strain energies of the products of these two reactions. The exo product **15b** has a strain energy of 35.4 kcal/mol, while the epimer **12b** is calculated to have only 31.3 kcal/mol of strain. In addition, the most stable conformation of the exo product **15b** correlates with the most stable conformation of the exo product **12b**. Thus, the epimerization is thermodynamically driven by the relief of about 4.1 kcal/mol

(10) (a) Maskill, H. *The Physical Basis of Organic Chemistry*; Oxford University Press: Oxford, 1985. (b) Zefirov, N. S. *Tetrahedron* **1977**, *33*, 2719.

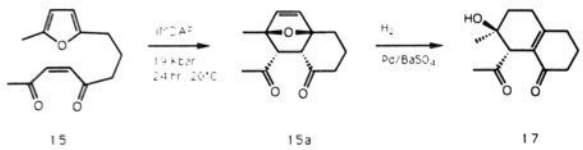

Figure 7. Product **15a** can be trapped under suitable conditions to afford **17**.

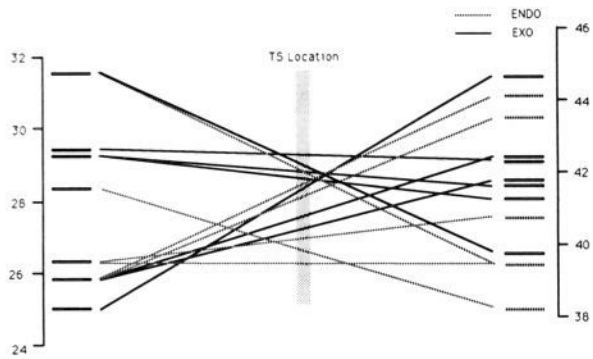

Figure 8. Correlation diagram for the reaction of compound **13**. Only the endo product was observed at 10 kbar. When the reaction was performed at 19 kbar, up to 20% of the exo product was observed.

of strain energy and should also be the kinetically most favorable fate for **15b**. Later studies involving hydrogenation of the crude reaction mixture obtained at 19 kbar further vindicated our model, since up to 30% of product **17** was observed. This product arises from ring opening of the initial endo adduct, as shown in Figure 7.

Although the reactions of **13** (trans dienophile) and **16** (cis dienophile) are closely related to the two previously discussed reactions, the correlation diagrams suggest that they should exhibit substantially different behavior. When we began the theoretical investigation, both reactions had been performed at 10 kbar. Under these conditions we obtained only the endo products **13a** and **16a**. Thermodynamic considerations of the products show that the observed product **16a** is predicted to be substantially more stable than **16b**, but we predicted that the unobserved product **13b** would be more stable than the observed product **13a**. Examination of the correlation diagrams (shown in Figures 8 and 9) suggested a kinetic explanation for the observed results. In both reactions, our axiomatic model predicts that the lowest-energy transition states should lead to endo products. The observation that neither reaction had proceeded substantially toward completion (≥50% SM for each reaction) under the reaction conditions is in complete agreement with the explanation that both reactions were operating under kinetic control. Based on our model, we predicted that if each reaction were run under conditions which would favor thermodynamic control, the reaction of **16** would still yield the endo product **16a** as the sole product but the reaction of **13** would show a product mixture in which the as yet unobserved exo product **13b** would eventually predominate.

When these reactions were run at 19 kbar, the greater consumption of starting material showed that the reaction had been driven further toward completion under these conditions, and thus it should demonstrate a greater degree of thermodynamic control. The experimental results[5] were in qualitative agreement with our predictions: the reaction of **16** still afforded only the endo product **16a** but the product mixture from **13** included 20% of **13b** and 80% of **13a**. The fact that the predicted preponderance of **13b** was not observed could be due to several factors: the model could be incorrect or the reaction might not have achieved thermodynamic equilibrium. Although 12% of the starting material **13** was recovered, it is not possible to say if this represents unreacted starting material or an equilibrium concentration of starting material. However, studies of these two reactions were difficult because the products were highly strained and prone to cycloreversion. Commonly, the adducts were trapped by hydrogenating

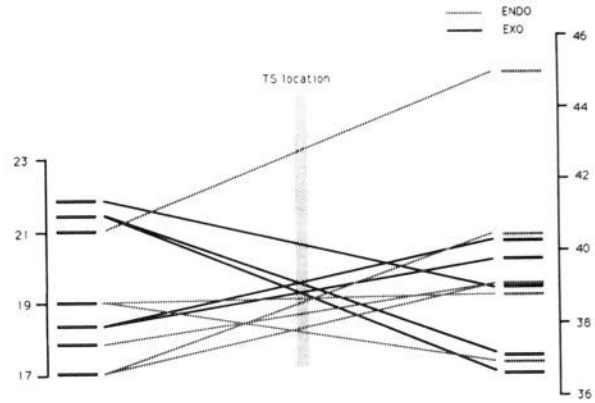

Figure 9. Correlation diagram for the reaction of compound **16**. Only the endo product was observed at 10 kbar and at 19 kbar.

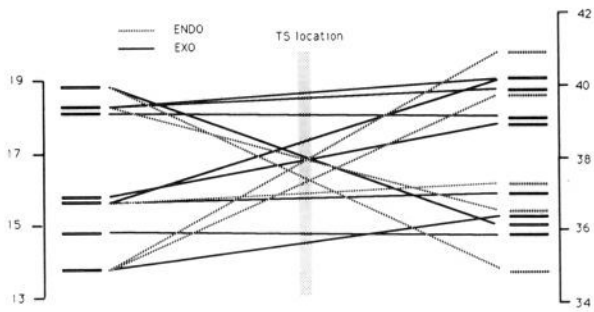

Figure 10. Correlation diagram for the reaction of compound **10**. At short reaction times, only the kinetic exo product is observed. Under longer reaction times, the thermodynamically favored endo product predominates.

the crude reaction mixture before it had time to undergo substantial reversion to starting materials. Thus, it was felt that it would be advantageous to study another substrate that showed a similar time-dependent product ratio but would be more experimentally tractable.

The reaction of **10** to afford **10a** and **10b** proved to meet these criteria, and so it was studied in greater detail. The correlation diagram for this reaction is shown in Figure 10. The endo product **10a** is predicted to be the thermodynamically favored product, while our model predicts that the two or three most stable transition states should lead to the exo product **10b**. When we began the theoretical investigation of this reaction, two data points were known: at very short times only **10b** was observed, while at 8 h an approximately equimolar mixture at **10a** and **10b** was observed. These experimental results are in agreement with our model, and after examining our model we predicted that the final equilibrium mixture should be approximately 4 endo to 1 exo. The reaction was run again, and the product and starting material concentrations were carefully examined at 4, 8, 24, and 50 h. These results are shown in Figure 11. The results clearly show that the exo product is the kinetically favored product, while the endo product is thermodynamically favored. The isolated mixture at 50 h is 70% endo and 25% exo, in good agreement with our model. The final equilibrium concentration of starting material **10** is approximately 5%, and this concentration is obtained long before the endo/exo ratio even begins to approach equilibrium. Thus, the presence of 12% starting material in the reaction of **13** to give **13a** and **13b** cannot be used as a measure of the degree of completion of that reaction or of achievement of equilibrium.

Before we turn from the examination of reactions of **11–16**, we need to address the failure of reactions of **11** and **14** to afford any appreciable amount of product under the reaction conditions. Examination of the correlation diagram for the reaction of **14** (Figure 12) leads to the prediction that the exo **14b** product should be observed. However, only traces of products were observed, and they could not be characterized. No products were observed for

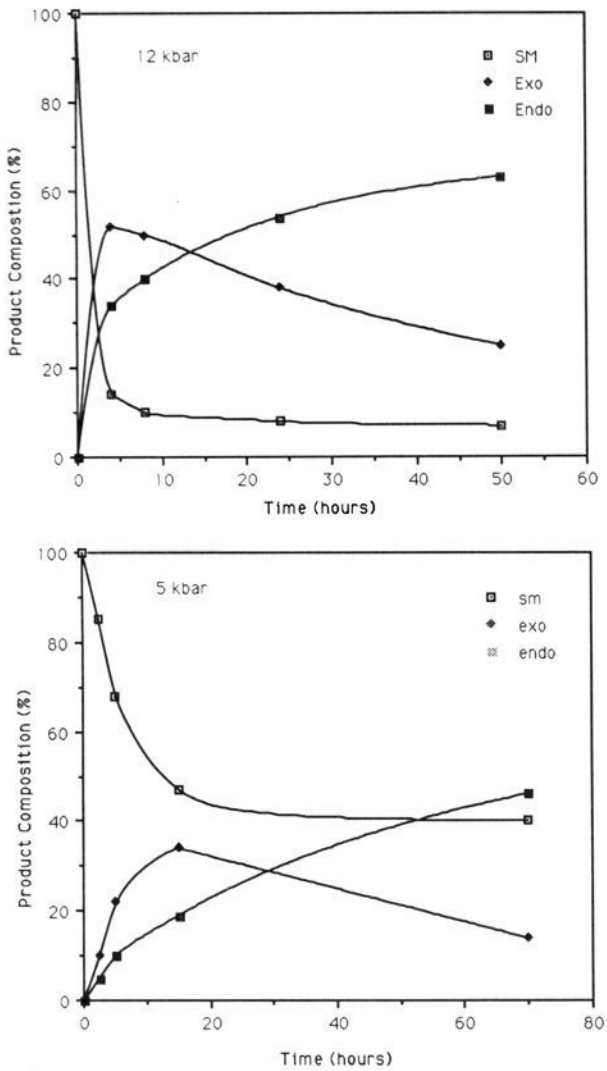

Figure 11. Plot of the concentrations of starting material (**10**), endo product (**10a**), and exo product (**10b**) as a function of time and pressure.

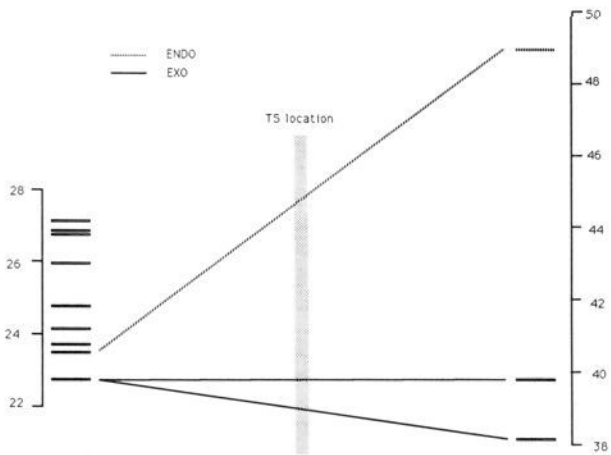

Figure 12. Correlation diagram for the reaction of compound **14**. Only traces of product were observed.

the reaction of **11**. Previously we demonstrated that the equilibrium direction of the reaction could not be correlated to the strain of the product nor to the overall ΔH_{strain} of the reaction computed from the most stable SM and product. However, if we plot the ΔH_{strain} of the most favorable *correlation pathway*, we see a strong trend, as shown in Figure 13. The reactions with

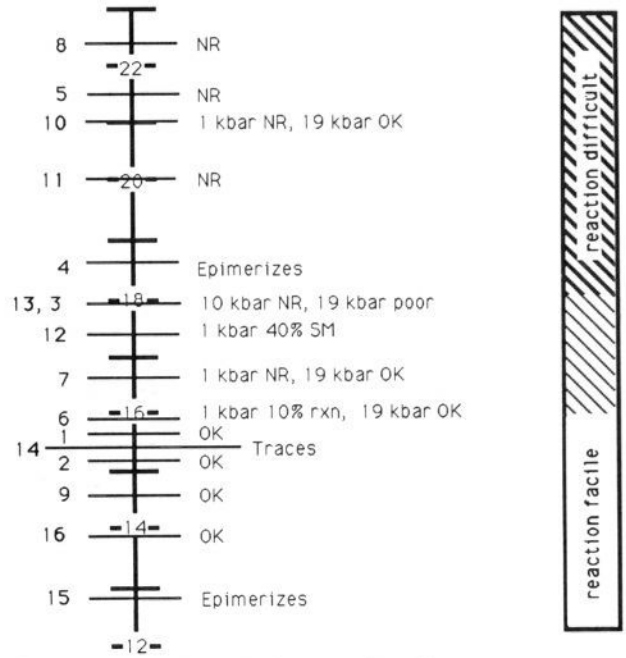

Figure 13. Plot of the ΔE of the most favorable correlation pathway versus reaction progress, displayed on an energy ladder. There is a strong trend from ΔE = 12 kcal (reactions are facile) to ΔE = 22 kcal (no reaction, NR).

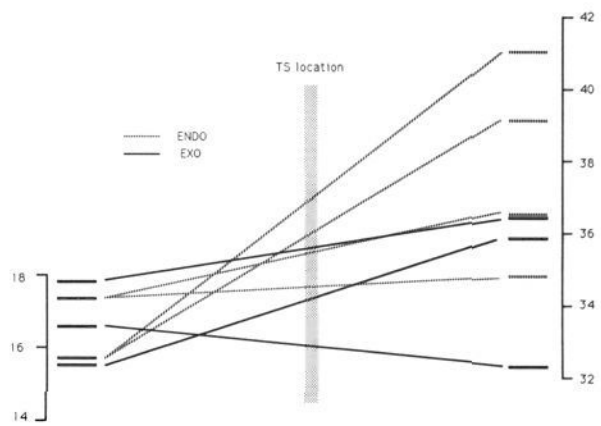

Figure 14. Correlation diagram for the reaction of compound **1**.

low ΔH_{strain} proceed readily at short times and lower pressures (1 bar to 10 kbar), while those with high ΔH_{strain} proceed with difficulty. At first glance, the reaction of **10** seems to be a deviation from this simple rule of thumb, but it should be remembered that this reaction required more than 50 h to *approach* equilibrium at 12 kbar, while the reactions of **5** and **11** were studied under far less rigorous conditions. This trend helps to explain the fact that while the products from reactions 5 and 8 are comparable in stability to the products from other successful reactions, no products were observed in these reactions.

Next we will examine the homologous series of reactions of compounds **1**–**4**. The correlation diagrams for these reactions are shown in Figures 14–17. In all of these cases, predictions based on our model are in agreement with experimental observations that the exo product was found as the major product. We performed a theoretical analysis of this reaction when all of the observations had been made at pressures of 10 kbar or less. At that time, examination of our model led us to make the following predictions. In all of these reactions, the ratio of $\Delta H^{\ddagger}_{exo}/\Delta H^{\ddagger}_{endo} < \Delta H_{exo}/\Delta H_{endo}$, thus indicating that the reaction will yield a higher amount of endo product when it is kinetically controlled than when it nears thermodynamic equilibrium. In the reaction of **1** at 10 kbar, the exo:endo ratio was 3:1 and a substantial

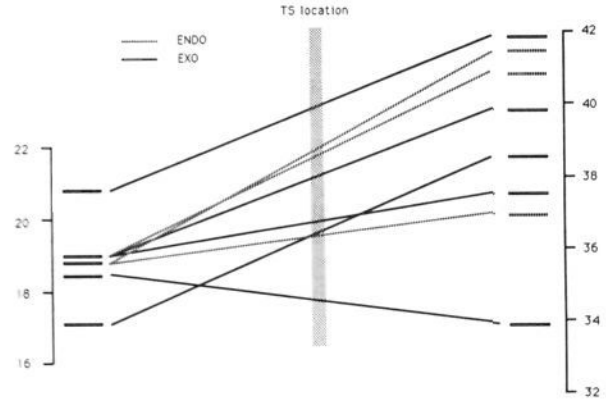

Figure 15. Correlation diagram for the reaction of compound **2**. Exo:endo ratio increased with more rigorous conditions, presumably due to greater amount of thermodynamic control.

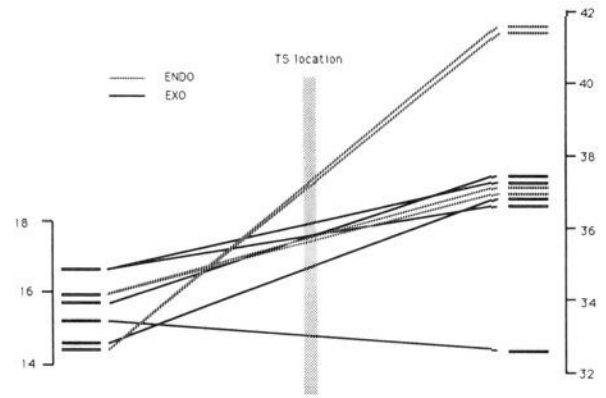

Figure 16. Correlation diagram for the reaction of compound **3**. Observed 19:1 exo:endo ratio.

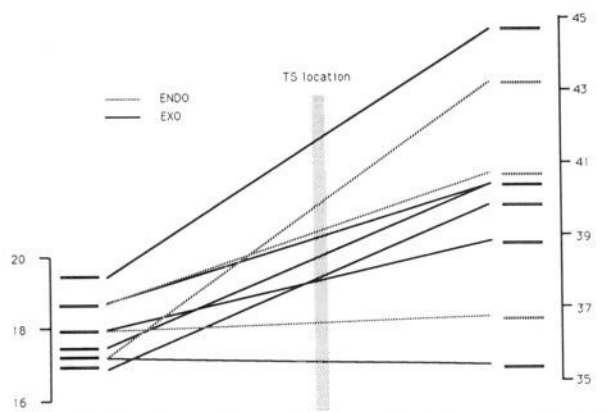

Figure 17. Correlation diagram for the reaction of compound **4**. Only the epimerization product **3b** was observed.

amount of starting material was recovered. We predicted that at higher conversions the exo:endo ratio would increase slightly. At 19 kbar, the ratio did increase to 7:2, but this small change might not be significant. Once again, the low consumption of starting material could indicate that the reaction is far from equilibrium and that given more time the ratio might still increase. In the reaction of **2**, the difference between the transition-state energy ratios and the product energy ratios is larger than in the reaction of **1**, leading to the prediction that there should be a larger increase in the exo:endo ratio than was observed in the reaction of **1**. In fact, when the reaction was carried out at 19 kbar, the ratio increased from 3:1 to 5:1. Reactions of **3** and **4** showed no reaction when initially studied at 10 kbar. Examination of the correlation diagrams in Figures 16 and 17 and of the energy chart in Figure 13 led to the prediction that while these reactions might

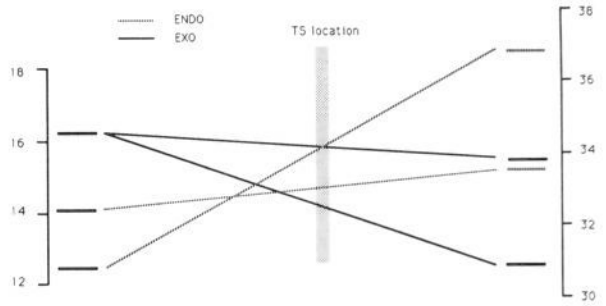

Figure 18. Correlation diagram for the reaction of compound **6**.

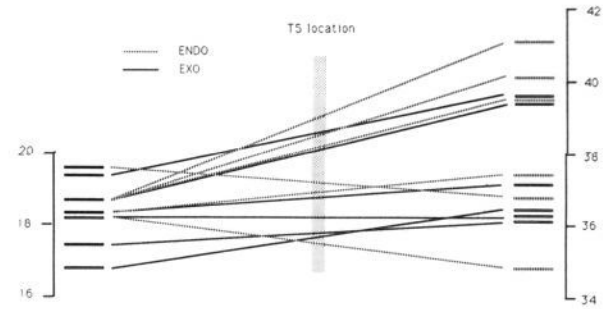

Figure 19. Correlation diagram for the reaction of compound **7**. The observed 1:1 ratio cannot be explained by relative product stabilities but is in good agreement with a kinetic explanation based on the correlation lines.

be recalcitrant, they should proceed under more rigorous conditions. We predicted that the reaction of **3** would give a much higher exo:endo ratio than either the reaction of **1** and **2**. In fact, when carried out at 19 kbar, the reaction of **3** afforded a 19:1 exo:endo ratio. Similarly, the reaction of **4** did proceed when run at 19 kbar, but the product was primarily **3b** with a variable amount of rearrangement products. No conclusions as to the exo:endo ratio of this specific DA reaction can be safely drawn, since **3b** can arise either from pre-DA isomerization of the *Z* double bond in SM **4** to give the *E* double bond in SM **3** (which would afford **3b** directly) or from post-DA epimerization of **4b** to give **3b**.

The next homologous series is that of compounds **5**–**7**. We have already demonstrated that our model would not predict any product from the reaction **5**, since the ΔH of the best correlation pathway is over 21 kcal/mol. In fact, under the experimental conditions tried, the reaction of **5** did not afford product. However, the best pathways for the reactions of compounds **6** and **7** are below 19 kcal/mol, and so these reactions were predicted to be feasible under slightly forcing conditions. Both reactions were found to be possible at higher pressures but not at lower pressures. Reaction of **6** demonstrated an 18:1 ratio of exo:endo products, which is in good agreement with the model based on the correlation diagram shown in Figure 18. Reaction of **7** demonstrated the need for considering the transition-state model instead of the relative energies of the products: the endo product **7a** is more stable than the exo product **7b** by 1.2 kcal/mol (>85:15), yet the experimentally observed ratio is 1:1. If we consider the relative energies of the transitions states on the basis of our correlation model, shown in Figure 19, we can see that a 1:1 kinetic ratio is easily explained. We would predict that the endo:exo ratio would approach 85:15 at longer reaction times or higher pressure, but this experiment has not been carried out.

The final series is reactions of compounds **8**–**10**. We have discussed reactions of **8** and **10** in previous paragraphs and shown that the model and the experimental results are in good agreement. Examination of the correlation diagram for the reaction of **9**, shown in Figure 20, suggests that although the exo product **9b** should be the major product, 20–40% of the endo product **9a** should be expected. In fact, only the exo product **9b** was observed by NMR. It is possible that WIZARD might have missed a

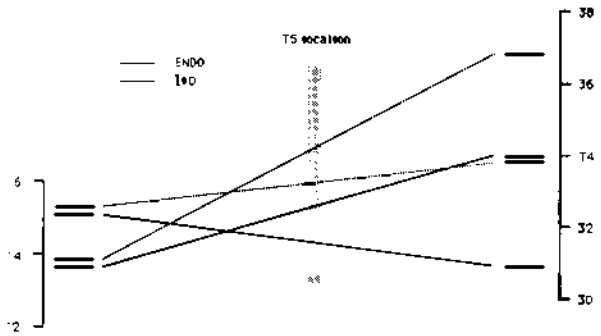

Figure 20. Correlation diagram for the reaction of compound **9**. The model is not in good agreement with the observation that only exo product is formed. Calculations predict that this reaction is among the most facile, and this reaction may be under considerable thermodynamic control.

low-lying conformation of **9h**. Although WIZARD has been shown to be comprehensive in all cases in which we have challenged it with Monte Carlo or other search methods, that does not constitute a rigorous proof that WIZARD cannot miss conformations. A brief Monte Carlo search[11] on the conformational space of **9b** turned up no new conformations. Another explanation might arise if we note that this reaction is fairly facile, being the third most facile reaction shown in Figure 13. If we invoke greater degrees of thermodynamic control for the reactions as they tend toward the bottom of the scale shown in Figure 13, then we have to consider the effect that this will have on the predictions for other reactions that should be affected. In fact, examination of the correlation diagrams suggests that we would obtain the same results for reactions of **t5** and **t6** (the two reactions of lower correlation path energy) while bringing the experimental results for reaction of **9** into agreement with the model. However, we are loath to make such a sweeping generalization on the basis of one experiment out of 16, and so we still consider this problem to be unresolved at this time.

(11) t5000 semirandom [number of atoms moved = rand · rand · t0 (where rand is random number from 0.0 to 1.0), equiprobable random *xyz* direction, distance = (−7.0 · rand) + 3.5 Å, hydrogens move with carbons] perturbations of the molecule, followed by MM2 minimization and duplicate search.

Conclusions

The axiomatic theory of the 1MDAF reactions is successful in modeling known experimental results and in the prediction of as yet unknown results. In 15 out of 16 cases, the model is in good quantitative agreement with experimental data. The model predicts the correct isomer for the remaining case, but the quantitative predictions vary from experiment by about 20–40%. The true strength of the model is shown by the fact that when the model disagreed with preliminary experimental results performed with short reaction times or low pressures, it was shown to be correct when the experiments were performed under more rigorous conditions. The model can be broken into two parts: the general methodology and the specific 1MDAF reaction model. Since the success of the study depends on the validity of each part, this study not only provides an insight into the 1MDAF reaction but also demonstrates the utility of the general method of implicit transition-state modeling. This technique will be useful for at least two reasons. First, this technique depends on well-proven and accepted techniques for conformational search and molecular modeling. Explicit modeling of transition states is difficult: ab initio methods require vast amounts of CPU time for molecules of this size, molecular mechanics parameters for the Houk method are currently available only for a limited number of transition states, and techniques for efficient explicit conformational searching of transition states are just now being developed. While we have utilized our WIZARD program to rapidly and systematically obtain all of the conformations for the starting materials and products, in principle one could utilize any other technique (Monte Carlo, distance geometry, torsion angle driving, etc.) to obtain these conformations, as long as the resulting sets of conformations are comprehensive. Second, the implicit method will be useful because it rapidly provides information on both the thermodynamic and the kinetic components of mixed reactions. This allowed us to understand and even predict the time-dependent nature of the 1MDAF reaction and should do so with future reactions.

Acknowledgment. D.P.D. wishes to acknowledge the donors of the Petroleum Research Fund, administered by the American Chemical Society, for partial support of this research and the Stardent Corporation for the support of this research through the grant of a Stardent Titan-II minisupercomputer. L.M.H. thanks Oxford University Research Support Scheme and I.C.I. Pharmaceuticals for financial support toward the purchase of the 20-khar high-pressure vessel.